

RSC Advances



This is an *Accepted Manuscript*, which has been through the Royal Society of Chemistry peer review process and has been accepted for publication.

Accepted Manuscripts are published online shortly after acceptance, before technical editing, formatting and proof reading. Using this free service, authors can make their results available to the community, in citable form, before we publish the edited article. This *Accepted Manuscript* will be replaced by the edited, formatted and paginated article as soon as this is available.

You can find more information about *Accepted Manuscripts* in the [Information for Authors](#).

Please note that technical editing may introduce minor changes to the text and/or graphics, which may alter content. The journal's standard [Terms & Conditions](#) and the [Ethical guidelines](#) still apply. In no event shall the Royal Society of Chemistry be held responsible for any errors or omissions in this *Accepted Manuscript* or any consequences arising from the use of any information it contains.

Cite this: DOI:

10.1039/c0xx00000xwww.rsc.org/xxxxxx

ARTICLE TYPE

Synthesis, *in vitro* evaluation and DNA interaction studies of *N*-allyl naphthalimide analogues as anticancer agents

Meenakshi Verma, Vijay Luxami and Kamaldeep Paul*

Received (in XXX, XXX) Xth XXXXXXXXX 20XX, Accepted Xth XXXXXXXXX 20XX

DOI: 10.1039/b000000x

Abstract: A novel series of 2-allyl-6-substituted-benzo[*de*]isoquinoline-1,3-diones has been synthesized and evaluated against 60 human tumor cell lines for their *in vitro* antitumor activities. Compound **6b** proved to be the most active member at single dose concentration of 10 μ M and broad spectrum of antitumor activity with GI₅₀, TGI and LC₅₀ values of 84.2 nM, 27.6 μ M and 89.3 μ M respectively at five dose concentration levels. DNA binding properties of this compound has been investigated by UV-Vis and fluorescence spectrophotometer as well as thermal denaturation experiments. Molecular docking studies of compound **6b** has also been supported the corresponding biological data.

1. Introduction

In the area of anticancer research, the development of small molecules capable of interacting with deoxyribonucleic acid (DNA) and exhibiting anticancer activities has received enormous attention in recent years.¹ Amongst these it has been found that 1,8-naphthalimides (benz[*de*]isoquinolin-1,3-diones) and its derivatives possess high anticancer activity towards various human and murine cells.²⁻⁷ The development of functional 1,8-naphthalimide derivatives as anticancer agents and DNA targeting is a fast growing area and has resulted in several such derivatives like amonafide, mitonafide, elinafide and bisnafide (Figure 1) that entered into clinical trials.⁸ Additionally the naphthalimide ring can also be substituted, for example, at the 3- or 4-position with amino, bromo or nitro groups. This not only allows the introduction of other active functional groups, which can be used for targeting biomolecules, but can have a major effect on the electronic properties with a consequent influence on the chemical, photochemical and spectroscopic properties. In literature, many examples are known where anticancer activities of naphthalimides have been significantly affected via fusing aromatic rings⁹⁻¹⁰ or varying the position and size of side chains.¹¹ Qian and co-workers have synthesized a series of naphthalimides with the substitution of 1,2,3-triazole ring at 3 or 4 position. These newly synthesized compounds showed better cytotoxic activity against breast cancer cell line MCF-7 than amonafide.¹²⁻¹³ Wang and co-workers have synthesized naphthalimide analogues substituted with amino acids, and dichloroacetamide functionalizations at 3-position and evaluated their cytotoxic activities against Hela, A549 and K562 cancer cell

lines.¹⁴ Another example of such modification is UNBS5162, which proved to be a good anticancer agent that presently at clinical trials. It showed lesser toxic side effects which decreased CXCL chemokine expression in advanced solid tumors or lymphoma.¹⁵ The probable mechanism of these anticancer activities of naphthalimide derivatives is supposed to be capable of either intercalation with base pairs or alkylation, or groove binding of DNA as the substituted naphthalimides are characterized by presence of planar chromophore portion.¹⁶ Thus, naphthalimides are not only interact with DNA, but members of this class also offer various sites for numerous modifications which provide a hope in the field of improvement of their antitumor activity.¹⁷ Synthesis of such analogues is the high priority for medicinal research because DNA is one of the important targets for cancer treatment.¹⁸ Inspired by its promising antitumor activities and keeping in mind for their possibility of DNA intercalation, we have decided to synthesize *N*-allyl naphthalimide analogues substituted with primary and secondary amines in order to improve their anticancer activities and selectivity profile. Calf thymus (ct)-DNA studies have also been performed with the most active compound of this series in order to observe its interaction with DNA.

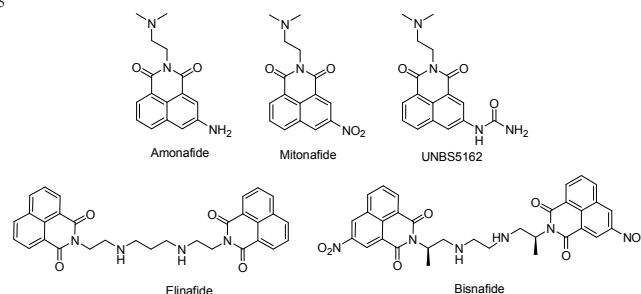


Figure 1 Chemical structure of some naphthalimide analogues

2. Results and Discussion

2.1. Chemistry

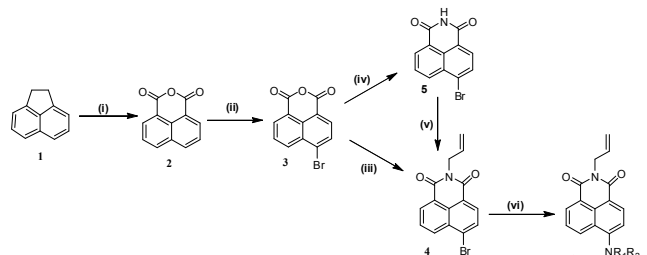
Target naphthalimide analogues **6a-n** has been prepared via multistep reactions using commercially available starting material acenaphthene (**1**) (Scheme 1). Oxidation of acenaphthene was done with acetic acid and sodium dichromate at 75 °C for 8 h to obtain 1,8-naphthalic anhydride (**2**) with 75% yield. Compound **2** was then treated with bromine in presence of KOH solution at 60 °C for 6 h to get white solid of 6-bromo-benzo[*de*]isochromene-1,3-dione (**3**) with 77% yield (m.p. = 117-119 °C). Refluxing of

School of Chemistry and Biochemistry, Thapar University, Patiala-147 001, India
*Corresponding author. Tel.: +91 9465670595; fax +91 175 236 4498 E-mail address: kpaul@thapar.edu (K. Paul)

† Electronic Supplementary Information (ESI) available: [NMR data]. See DOI: 10.1039/b000000x/

compound **3** with allylamine in the presence of ethanol for 8 h resulted in the formation of white solid of 2-allyl-6-bromo-benzo[de]isoquinoline-1,3-dione (**4**) in 80% yield (m.p. = 128–130 °C).

Scheme 1^a Synthesis of 2-allyl-6-substituted -benzo[de]isoquinoline-1,3-dione



Reagents and conditions^a (i) acetic acid, Sodium dichromate, 75 °C, (ii) potassium hydroxide, bromine, 60 °C, (iii) allyl amine, ethanol, reflux, (iv) NH₄OH, ethanol, reflux, (v) allyl bromide, EtOH, reflux, (vi) NHR₁R₂, K₂CO₃, TBAHSO₄, acetonitrile, reflux.

Table 1 Physical data of synthesized compounds

Entry	NR ₁ R ₂	Product	Time (h)	Yield (%)	m.p. (°C)
1	piperidin-1-yl	6a	9	78	115-117
2	morpholin-4-yl	6b	8	87	173-174
3	pyrrolidin-1-yl	6c	9	76	155-158
4	4-amino-benzenethiol	6d	11	60	185-188
5	2-amino-benzenethiol	6e	12	59	205-208
6	2-amino-pyridin-3-ol	6f	10.5	63	210-212
7	5-bromo-pyridin-2-ylamine	6g	10	53	205-207
8	2-amino-ethanol	6h	8.5	57	-
9	allylamine	6i	9	50	-
10	n-propylamine	6j	8.5	65	-
11	n-butylamine	6k	8	62	-
12	n-pentylamine	6l	8.5	59	-
13	n-hexylamine	6m	9	51	-
14	n-octylamine	6n	8	49	-

Alternatively, compound **4** was also synthesized by the refluxing compound **3** with ammonium hydroxide in ethanol to get 6-bromo-benzo[de]isoquinoline-1,3-dione (**5**) followed by treatment with allyl bromide in the presence of ethanol at reflux condition for 8 h. The crude product was purified through column chromatography to get pure 2-allyl-6-bromo-benzo[de]isoquinoline-1,3-dione (**4**) in 65% overall yield. Compound **4** was further refluxed with primary and secondary amines in the presence of K₂CO₃ and CH₃CN using TBAHSO₄ as catalyst for 8-12 h to get the crude product. The crude was purified by column chromatography to afford pure target product 2-allyl-6-substituted-benzo[de]isoquinoline-1,3-dione (**6a-n**) in moderate to good yields (Table 1). Structures of all these final compounds were confirmed by ¹H and ¹³C NMR as well as mass spectrometry (Supporting Information).

2.2. *In vitro* screening for antitumor activities

All compounds were submitted to National Cancer Institute (NCI) for evaluation of their *in-vitro* antitumor activities.¹⁹⁻²¹ Compounds **6b-c** and **6f-i** were evaluated against 60 human cell

lines at single dose concentration of 10 μM which includes nine tumor subpanels and their output was reported as a mean graph of the percent growth of the treated cells and presented as percentage growth inhibition (GI %). Compound **6b** exhibited significant growth inhibition and evaluated as 60 cell panels at five dose concentration levels.

Preliminary *in vitro* antitumor screening revealed that only compounds belonging to secondary amines especially morpholine showed significant inhibition for almost all the cancer cell lines. The percentages of inhibition for these cancer cells were more than 60% of tested derivative while primary amines substituted **6f-i** showed weak activities with percentages of inhibition less than 40% except few cell lines (Table 2). These variations could be correlated to the difference in C6 substituents on the core naphthalimide moiety, in which the presence of morpholine moiety is an important factor affecting for antitumor activity. On the contrary, compound **6c** with pyrrolidine, showed potency towards non-small lung cancer cell line EKVX and renal cancer cell line A498 with GI values of 40.31% and 33.55% respectively. In series of primary amines **6f-i**, significant growth inhibitions were observed for renal cancer cell (UO-31; 26.10–32.85%), lung cancer cell (HOP-92; 21.32–50.37%) and prostate cancer cell (PC-3; 23.41–39.40%). Compound **6i** with allylamine at C6 position also showed selectivity towards lung cancer cell line HOP 92 and breast cancer cell line MCF 7 with GI values of 50.37% and 66.05% respectively. On the other hand, naphthalimide analogue **6b** proved to be the most active compound of these series. It showed broad spectrum of activity against all nine subpanels of cancer cell lines at primary single dose concentration level (Table 3).

Table 2 Percentage growth inhibition (GI%) of the selected compounds over the most sensitive tumor cell lines at single concentration of 10 μM

Cell lines	6c	6f	6g	6h	6i
MOLT-4	-	-	27.75	-	-
RPMI-8226	-	-	21.90	-	-
SR	22.00	25.51	20.73	-	25.25
EKVX	40.31	31.68	-	-	-
HOP-92	28.67	36.81	43.52	21.32	50.37
NCI-H522	24.02	-	-	-	-
HCT-116	-	25.75	22.83	-	-
SNB-75	-	30.78	24.71	-	-
UACC-62	21.85	28.97	-	-	24.18
OVCAR-4	-	22.66	-	-	-
A498	33.55	-	-	-	-
CAKI-1	-	31.16	34.13	20.17	27.05
UO-31	-	26.10	32.85	27.36	28.50
PC-3	23.41	39.40	28.38	25.20	30.66
MCF7	-	-	-	-	66.05
MDA-MB-231/ATCC	-	34.58	23.72	-	-
T-47D	25.27	29.71	-	-	-
MDA-MB-468	-	-	-	-	39.71

From the above data, it is clear that compound **6b** is the most active member of the series. Consequently, this active compound was carried over and tested against a panel of different tumor cell lines at five dose concentration level (Figure S31-S34) where it exhibited remarkable anticancer activity against non-small cell lung cancer cell line HOP-92, CNS cancer cell line SNB-75 and breast cancer cell line HS 578T with GI₅₀ values in the nano molar range. Compound **6b** also showed specificity towards central nervous system (CNS), melanoma, renal and breast cancer

Table 3 The percentages of growth inhibition of compound **6b** over the full panel of tumor cell lines at a single concentration of 10 μM

Subpanel Cell lines	Inhibition (%)	Subpanel Cell lines	Inhibition (%)
Leukemia		Ovarian Cancer	
CCRF-CEM	-7.18	IGROV1	-14.55
HL-60(TB)	-5.15	OVCAR-3	-66.42
K-562	90.22	OVCAR-4	85.64
MOLT-4	-21.21	OVCAR-5	78.58
RPMI-8226	-25.79	OVCAR-8	79.30
SR	-9.38	NCI/ADR-RES	93.94
Non-Small Cell Lung Cancer		SK-OV-3	86.12
A549/ATCC	96.95	Renal Cancer	
EKVX	-7.17	786-0	73.84
HOP-62	73.56	A498	-57.04
HOP-92	78.89	ACHN	81.42
NCI-H226	-2.43	CAKI-1	-39.46
NCI-H23	91.99	RFX 393	-29.91
NCI-H322M	-56.58	SN12C	83.04
NCI-H460	91.48	TK-10	-12.91
NCI-H522	-1.11	UO-31	-3.07
Colon Cancer		Melanoma	
COLO 205	-21.78	LOX IMVI	98.87
HCC-2998	-33.96	MALME-3M	-3.28
HCT-116	-25.42	M14	99.61
HCT-15	-9.11	MDA-MB-435	99.64
HT29	93.24	SK-MEL-2	-28.12
KM12	-56.35	SK-MEL-28	94.33
SW-620	92.76	SK-MEL-5	-62.71
CNS Cancer		UACC-257	-3.63
SF-268	-23.87	UACC-62	-24.66
SF-295	97.13	Breast Cancer	
SF-539	99.50	MCF7	-0.41
SNB-19	75.05	MDA-MB-231/ATCC	76.09
SNB-75	87.23	HS 578T	95.42
U251	94.63	BT-549	-47.77
Prostate Cancer		MDA-MB-468	-40.05
PC-3	-21.28	T-47D	-2.10
DU-145	89.72		

Table 4 Compounds **6b**, naphthalimide analogue and oxaliplatin of median growth inhibitory (GI_{50} , μM), total growth inhibitory (TGI, μM) and median lethal concentrations (LC_{50} , μM) of *in vitro* subpanel tumor cell line

Compds.	Activity	I	II	III	IV	V	VI	VII	VIII	IX	MG-MID ^a
6b	GI_{50}	0.098	0.115	0.112	0.043	0.073	0.132	0.072	0.095	0.018	0.084
	TGI	^b	21.3	17.04	10.53	15.61	40.18	33.42	7.174	3.962	27.69
	LC_{50}	^b	97.35	^b	92.41	87.55	80.14	89.48	^b	^b	89.38
Naphthalimide analogue	GI_{50}	2.90	3.94	6.58	4.09	6.93	6.97	3.30	3.23	5.20	5.05
	TGI	44.51	32.51	60.81	45.41	35.07	37.44	15.41	17.9	45.98	38.71
	LC_{50}	^b	93.94	98.84	93.98	83.93	97.94	88.94	80.15	^b	^b
Oxaliplatin	GI_{50}	0.844	20.86	2.58	8.91	3.50	11.76	6.61	13.13	42.96	12.35
	TGI	15.84	31.11	44.17	55.87	38.18	42.12	40.24	59.62	6.30	37.05
	LC_{50}	^b	79.40	73.96	63.10	72.07	^b	79.40	^b	^b	73.58

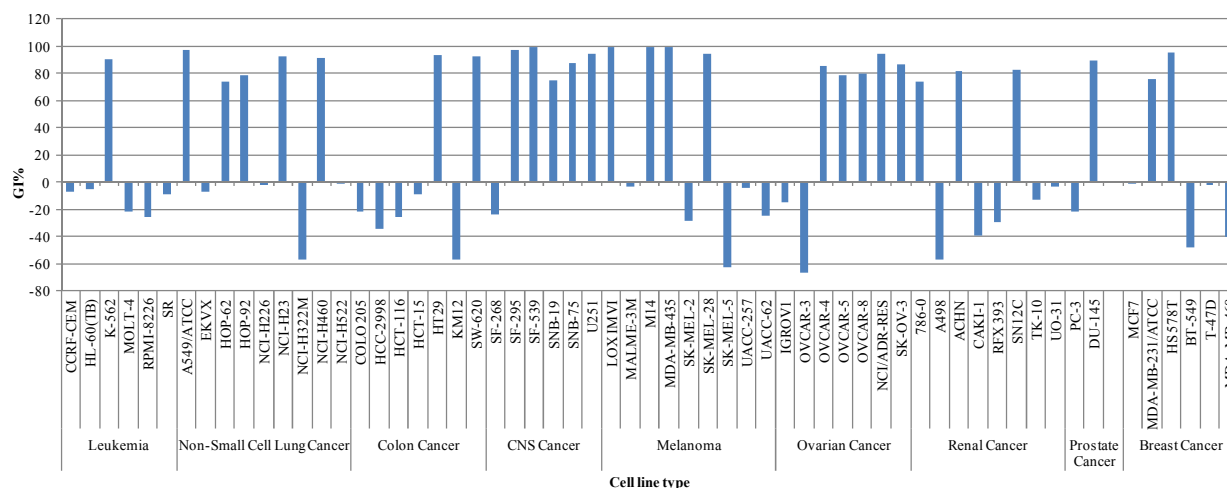
I, leukemia; II, non-small cell lung cancer; III, colon cancer; IV, central nervous system (CNS) cancer; V, melanoma; VI, ovarian cancer; VII, renal cancer; VIII, prostate cancer; IX, breast cancer.

^a Full panel mean-graph midpoint (μM)

^b Compounds showed values $>100 \mu\text{M}$

cell lines with GI_{50} values in the range of 18 nM-73 nM (Table 4, Figure 2). Compound **6b** also showed almost sixty fold more activity than naphthalimide derivative 3-(4-amino-phenylsulfanyl)-benzo[*de*]benzo[4,5]imidazo[2,1-*a*]isoquinolin-7-one,¹⁰ with MG MID GI_{50} , TGI and LC_{50} values of 84.2 nM,

27.6 μM and 89.3 μM respectively. Compound **6b** was also compared with approved chemotherapeutic drug, oxaliplatin²² which also showed interaction with DNA (Table 4). It was observed that compound **6b** showed almost one forty seven fold more activity than oxaliplatin (MG MID GI_{50} , TGI and LC_{50} values of 12.35 μM , 37.05 μM and 73.58 μM respectively). It is

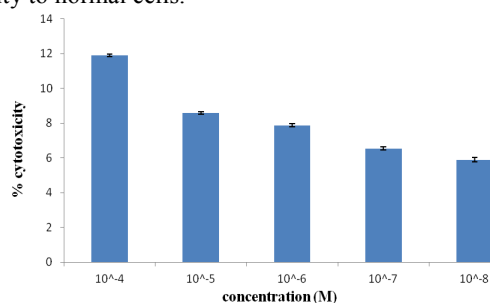


5 **Figure 2** The percentage growth inhibition (GI%) of compound **6b** over the full panel cancer cell lines at concentration of 10 μM

clear that replacement with morpholine group at C6 position than other secondary or primary amines, and allyl group at N2 position leads to excellent increase in antitumor activity.

2.3. Cytotoxicity (MTT and LDH)

10 Cytotoxicity of compound **6b** in human normal cell line (Hek293) was performed by means of a colorimetric assay (MTT assay). The results showed that there was only 12%, 8.5%, 8%, 6.5% and 6% cytotoxicity of compound **6b** to Hek293 cells at 10^{-4} , 10^{-5} , 10^{-6} , 10^{-7} and 10^{-8} M concentrations, 15 respectively (Figure 3). Compound **6b** showed only 12% toxicity to Hek293 cells even at 100 μM . These indicated that compound **6b** showed potent anticancer activity and low toxicity to normal cells.



20 **Figure 3** Effect of compound **6b** on Hek 293 cells

Lactate dehydrogenase (LDH) leakage is an indicator of cell membrane integrity.²³ When the cell membrane is disrupted, the membrane-bound LDH leaks into the medium and hence, LDH leakage is considered a hallmark of cytotoxicity. Cell death leads to a collapse in membrane integrity, thereby releasing LDH into the medium. In the present study, a significant level of LDH leakage was observed in the cell culture medium of the A549 cell line at 25 one (IC_{50}) and two doses ($2\times\text{IC}_{50}$), when they were treated with the respective IC_{50} concentrations of the compound for a period of 12 h and 24 h (Figure 4). It has been suggested that compound **6b** exhibited significant membrane-damaging 30

effects showed selectivity towards cancer cells while 35 exhibiting minimal/no toxicity towards normal cells.

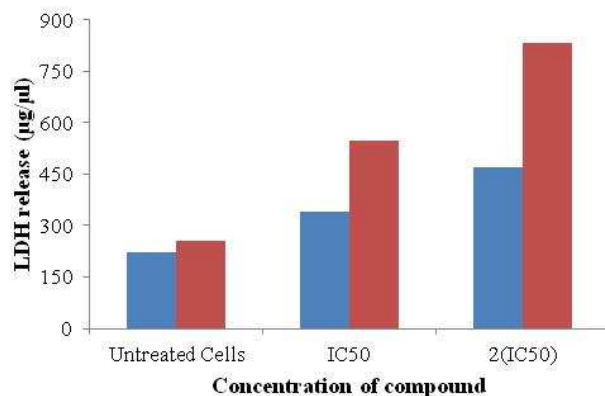


Figure 4 LDH release of compound **6b** at one and two doses after 12 h (blue bar) and 24 h (red bar).

2.4. DNA binding studies

40 DNA binding studies of the most active compound **6b** has been evaluated using both UV-Visible and fluorescence spectrophotometer in order to determine the interaction of compound with ct-DNA.²⁴ The addition of ct-DNA (4-100 μM) to the phosphate buffered solution of **6b** (20 μM) caused 45 decrease in absorption intensity at 405 nm (Figure 5).

Fluorescence titrations were also performed with ct-DNA in phosphate buffered solution of compound **6b**. The incremental addition of ct-DNA caused emission enhancement with concomitant blue shift of emission band 50 from 555 nm to 520 nm. The apparent binding constant of **6b** with ct-DNA was determined to be $\log \beta = 5.03$ calculated from titration data using Benesi-Hildebrand method which is comparable with amonafide having $\log \beta = 5.15$. The intercalative nature of compound **6b** with ct-DNA has been 55 additionally supported by thermal denaturation experiment. Intercalation of molecules into the double helix is known to stabilize the DNA against thermal strand separation and thus increases thermal melting temperature (T_m).²⁵ The derivative

melting curve shows an increase of 18.2 °C in thermal melting temperature of ct-DNA (60 °C) upon addition of **6b** (78.2 °C). Thus, both UV-Visible and fluorescence titrations as well as thermal denaturation experiments indicated intercalative nature of compound **6b** with ct-DNA.

2.5. Ethidium bromide (EtBr) displacement study

In order to prove the reversibility of the compound **6b**:DNA complex, fluorescence quenching experiments of ethidium bromide:DNA were carried out by adding 0–20 μM of the compound to samples containing 10 μM EtBr, 10 μM DNA and a phosphate (pH = 7). Before the measurements, the system was shaken and incubated at room temperature for ~5 min. The emission was recorded at 100–750 nm. On addition of 100 μM solution of ethidium bromide to compound **6b**:DNA complex, the emission band at 520 nm disappeared with reappearance of the fluorescence maxima at 610 nm typically due to EtBr:DNA complex. It confirmed the reversible binding of ligand to DNA (Figure S35).

Competitive ethidium bromide binding studies were carried out in order to examine the binding mode of each complex with ct-DNA. The emission spectra of EtBr bound to ct-DNA in the absence and presence of each complex have been recorded at [EtBr] = 10 μM, [DNA] = 10 μM. The

emission intensities of EtBr bound to ct-DNA at 610 nm enhanced indicating that they cannot effectively displace EtBr from the EtBr:DNA complex (Figure S36). This observation is often considered to be due to that they can bind weakly to the DNA, probably by electrostatic interactions. It is generally agreed that strong fluorescence enhancement accompanies intercalation of the dye into the double helix conformation of the nucleic acid, but there is also evidence for additional non-intercalative, less fluorescence-enhanced sites, which are presumed to involve electrostatic binding.²⁶

2.6. ADME Prediction

In order to determine the properties and drug-like characteristics of compounds **6b-c** and **6f-i**, we carried out the calculation with Molinspiration software of the lipophilicity (expressed as the octanol/water partition coefficient and herein called logP), and the theoretical prediction of other ADME properties (molecular weight, TPSA, number of hydrogen donors and acceptors, and volume) for Lipinski's rule of five. Drug likeness seems to be a promising standard for the properties of a molecule which influences its pharmacodynamics and pharmacokinetics.²⁷ This rule is based upon the prediction that if a molecule have molecular weight ≤ 500, log P ≤ 5, ≤ 5 hydrogen bond donor sites and ≤ 10 hydrogen bond acceptor sites (N or O atoms), only then it can be accepted as a member of biological active drug family.²⁸

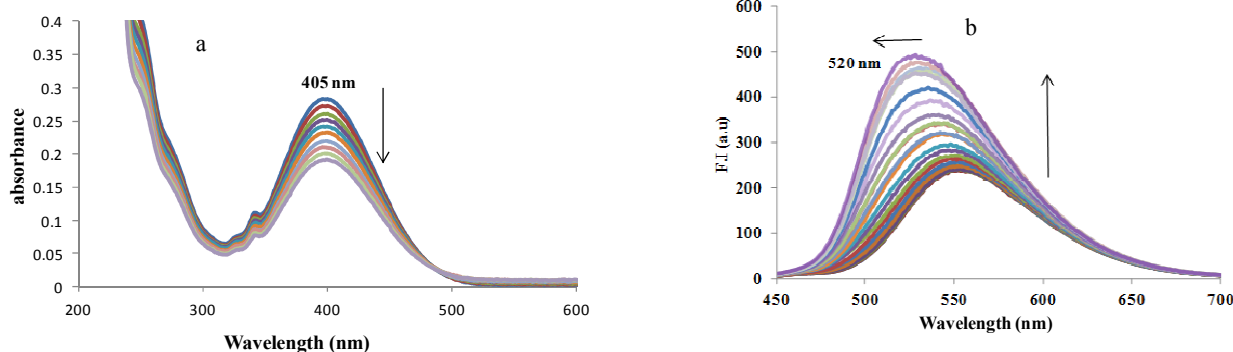


Figure 5 Effect of addition of ct-DNA (4–100 μM) on (a) absorption (b) emission spectra of compound **6b** (20 μM, pH 7.0) in phosphate buffer

Not considering this criteria may lead the poor absorption or permeation of the drug like molecule. Compounds selected for *in vitro* anticancer studies showed good physicochemical properties having no violation with any of the parameters. The results obtained are concluded in table 5. A comparison among the values leave us with the result that higher activity of compound **6b** may be described on the basis of lower value of log P factor,

Table 5 Structural properties of 2-allyl-6-substituted-benzo[de]isoquinoline-1,3-dione **6b-c** and **6f-i**, and the reference compounds.

Compds	m.wt.	logP	TPSA	nON	nOHNH	nviolations	volume
6b	322.36	2.60	51.54	5	0	0	294.65
6c	306.36	3.15	42.31	4	0	0	285.67
6f	345.35	3.47	84.22	6	2	0	300.15
6g	408.25	4.72	63.99	5	1	0	310.01
6h	296.32	1.87	71.33	5	2	0	266.50
6i	292.33	3.15	51.10	4	1	0	275.04
Amonafide	283.33	1.11	68.33	5	2	0	258.74
Naphthali mide	393.47	4.90	60.40	4	2	0	333.61

analogue¹⁰

which is an estimate of compound's overall lipophilicity (supported by low lipophilicity of amonafide). This parameter might be influence the factors like solubility and permeability through biological membrane.

2.7. Molecular docking studies

Molecular docking is an interesting tool to predict the possible drug–DNA interactions because the mode of action of various drugs like anticancer, antiviral, antibacterial, is directly associated with their binding to DNA.²⁹ To explore the most feasible binding site, interaction mode and binding affinity docking studies have been performed on compound **6b** with DNA (PDB ID: 1BNA).³⁰ Most stable binding conformation of **6b** fits into the major groove comfortably without disrupting the double helical structure of DNA and stabilized by electrostatic interaction. The planarity of naphthalimide core is comfortable for strong π–π stacking interactions and fits inside the DNA strands by van der Waals interaction and hydrophobic contacts

while morpholine moiety moved outside of the DNA strand (Figure 6). These results are consistent with UV-Vis and fluorescence studies. Therefore, docking of compound **6b** with DNA indicated the probable mode of action for anticancer activities.

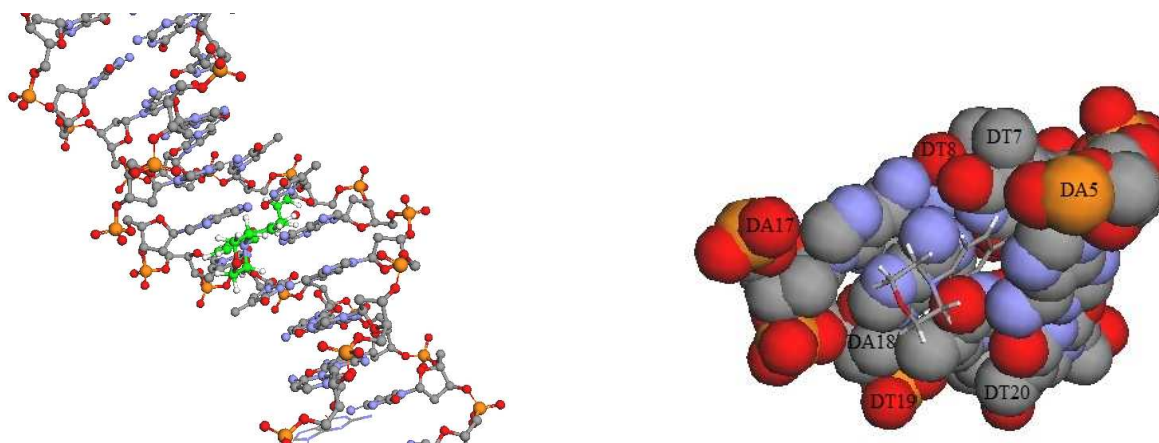


Figure 6 Molecular docked model of compound **6b** with DNA (pdb ID 1BNA)

3. Conclusion

The present work has led to the development of novel *N*-allyl naphthalimide analogues with different substitution of primary and secondary amines at C6 position. These compounds were evaluated towards 60 human tumor cell lines for their *in vitro* activities and some of which shown promising antitumor activities. Compound **6b** showed more active in most of the cancer cell lines at 10 μM concentration range and showed broad spectrum of antitumor activity with MG MID GI₅₀ value of 84 nM at five dose concentration levels. LDH leakage into the medium also confirmed the cytotoxic effect of this compound. Compound **6b** showed strong intercalating properties with ct-DNA determined by UV-Visible and fluorescence spectroscopy. Molecular docking studies indicating considerable interactions of these compounds with DNA that also favor the intercalation of synthesized compounds. These preliminary encouraging results of biological screening could offer an excellent framework in this field and thus further studies of these molecules are in progress.

4. Experimental

4.1. Chemistry

All chemicals and solvents of commercial grade were used without further purification and were supplied by spectrochemicals and Sigma-Aldrich. Melting points were determined in open capillaries and were uncorrected. ¹H and ¹³C NMR spectra were recorded on Jeol ECS-400 MHz spectrometer at 400 MHz and 100 MHz respectively, using CDCl₃ as solvent. The chemical shifts were expressed in parts per million with TMS as internal reference and *J* values are given in Hz. Mass Spectra of the synthesized compounds were recorded at Waters Micromass Q-ToF Micro. Elemental Analysis has been done with Thermo Scientific (Flash 2000) analyzer. UV-Visible spectra were recorded using Chamnion UV/Vis spectrometer. Fluorescence measurements were performed on a Varian Cary Eclipse fluorescence spectrometer. Thermal denaturation experiments were performed on Shimadzu UV-2450. Reactions

were monitored by thin layer chromatography (TLC) with silica plate coated with silica gel HF-254 and column chromatography was performed with silica gel mesh size 60-120. Hexane: ethylacetate were adopted solvent systems.

4.2. General procedure for synthesis of 2-allyl-6-bromo-benzo[*de*]isoquinoline-1,3-dione (**4**)

Sodium dichromate (14.50 g, 55.34 mmol) was added to a solution of acenaphthene (3 g, 19.7 mmol) and acetic acid (60 ml) with continue stirring at room temperature. This suspension was then heated to 75 °C for 8 h. Reaction was monitored with TLC. On complete reaction, cold water was added to the reaction mixture, resulted in precipitation. After filtration and washed off with water, yellow coloured solid of 1,8-naphthalic anhydride (2.9 g, 75%, m.p. 266-268 °C) **2** was collected and vacuum dried. A solution of 1,8-naphthalic anhydride (2.57 g, 12.9 mmol) and hot KOH (3.5 g in 15 ml water) was prepared and cooled to room temperature. To this solution, bromine was added drop-wise with vigorous stirring. After complete addition, reaction mixture was heated to 60 °C for 6 h. The resulted solution was acidified with HCl. Brown coloured solid separated out and filtered. This solid residue was further heated with 60 ml of 5% NaOH solution, filtered and treated with HCl solution till complete neutralization. Off white precipitates separated out, filtered and washed with cold water, dried to get off white solid of 6-bromo-benzo[*de*]isochromene-1,3-dione (**3**) (2.75 g, 77%, m.p. 117-119 °C). 6-Bromo-benzo[*de*]isochromene-1,3-dione (3.00 g, 10.8 mmol) was then reacted with allylamine (0.62 g, 10.8 mmol) in ethanol at reflux temperature for 8 h. After the completion of reaction (TLC), cooled the reaction mixture to get crude solid, filtered and washed with ethanol to afford pure white compound of 2-allyl-6-bromo-benzo[*de*]isoquinoline-1,3-dione (2.4 g, 80%, m.p. 128-130 °C) (**4**).

An alternative method for synthesizing 2-allyl-6-bromo-benzo[*de*]isoquinoline-1,3-dione has also been followed where 6-bromo-benzo[*de*]isochromene-1,3-dione (**3**) (2.00 g, 7.20 mmol) was refluxed with ammonium hydroxide (21.6 mmol) and ethanol. The reaction mixture was then cooled and solid product

was filtered to get 6-bromo-benzo[de]isoquinoline-1,3-dione **5** (m.p. 134-136 °C). **5** (7.25 mmol) was further refluxed with allylbromide (7.50 mmol) in presence of EtOH to yield crude product, washed with ethanol to get white solid of 2-allyl-6-bromo-benzo[de]isoquinoline-1,3-dione (**4**) (1.5 g, 65% overall, m.p. 128-130 °C).

2-Allyl-6-bromo-benzo[de]isoquinoline-1,3-dione (**4**)

White solid (80 %); m.p. 128-130 °C; ¹H NMR (400 MHz, CDCl₃): δ 8.66 (dd, ²J = 7.32 Hz, ³J = 0.92 Hz, 1H, ArH), 8.56 (dd, ²J = 8.68 Hz, ³J = 0.92 Hz, 1H, ArH), 8.41 (d, ²J = 7.80 Hz, 1H, ArH), 8.04 (d, ²J = 7.76 Hz, 1H, ArH), 7.86 (dd, ²J = 8.24 Hz, ³J = 0.92 Hz, 1H, ArH), 6.04-5.94 (m, 1H, CH), 5.35-5.30 (dq, ²J = 17.4 Hz, ³J = 1.36 Hz, 1H, CH₂), 5.24-5.20 (dq, ²J = 10.3 Hz, ³J = 1.36 Hz, 1H, CH₂), 4.80-4.78 (dt, ²J = 5.96 Hz, ³J = 1.36 Hz, 2H, N-CH₂); ¹³C NMR (100 MHz, CDCl₃): δ 163.3 (C=O), 133.4, 132.2, 131.9, 131.4, 131.1, 130.6, 130.5, 129.0, 128.1, 123.0, 122.1, 117.9 (ArC), 42.6 (N-CH₂); MS (EI) : m/z 316.0 (M⁺+1). Anal. Calc. for C₁₅H₁₀BrNO₂: C, 56.99; H, 3.19; N, 4.43. Found: C, 56.71; H, 3.33; N, 4.59.

4.3. General procedure for synthesis of 2-allyl-6-substituted-benzo[de]isoquinoline-1,3-dione (**6a-n**)

A mixture of 2-allyl-6-bromo-benzo[de]isoquinoline-1,3-dione (0.20 g, 0.65 mmol) and corresponding amine (0.80 mmol) was refluxed for 8-12 h in the presence of potassium carbonate (0.059 g, 1.05 mmol), TBAHSO₄ (catalytic amount) in acetonitrile. After completion of reaction, reaction mixture was extracted with chloroform, separated the organic layer, dried over Na₂SO₄, filtered and concentrated to get solid crude product of 2-allyl-6-substituted-benzo[de]isoquinoline-1,3-dione (**6a-n**) which were purified using column chromatography on silica gel using hexane:ethylacetate as eluents.

2-Allyl-6-piperidin-1-yl-benzo[de]isoquinoline-1,3-dione (**6a**)³¹

Yellow solid (78 %); m.p. 115-117 °C; ¹H NMR (400 MHz, CDCl₃): δ 8.59 (dd, ²J = 7.36 Hz, ³J = 1.40 Hz, 1H, ArH), 8.51 (d, ²J = 8.24 Hz, 1H, ArH), 8.40 (dd, ²J = 8.24 Hz, ³J = 1.36 Hz, 1H, ArH), 7.70 (dd, ²J = 8.72 Hz, ³J = 1.32 Hz, 1H, ArH), 7.19 (d, ²J = 8.24 Hz, 1H, ArH), 6.03-5.95 (m, 1H, CH), 5.32-5.27 (dq, ²J = 17.2 Hz, ³J = 1.40 Hz, 1H, CH₂), 5.20-5.17 (dq, ²J = 10.32 Hz, ³J = 1.36 Hz, 1H, CH₂), 4.81-4.78 (dt, ²J = 5.52 Hz, ³J = 1.36 Hz, 2H, N-CH₂), 3.24 (t, ²J = 5.04 Hz, 4H, pip-CH₂), 1.91-1.86 (m, 4H, pip-CH₂), 1.75-1.71 (m, 2H, pip-CH₂); ¹³C NMR (100 MHz, CDCl₃): δ 164.3 (C=O), 163.8 (C=O), 157.3, 132.8, 132.4, 131.1, 130.7, 129.9, 126.2, 125.3, 122.9, 117.1, 115.7, 114.6 (ArC), 54.4 (pip-NCH₂), 42.1 (N-CH₂), 26.1 (pip-CH₂), 24.3 (pip-CH₂); MS (EI) : m/z 321.1 (M⁺+1). Anal. Calc. for C₂₀H₂₀N₂O₂: C, 74.98; H, 6.29; N, 8.74. Found: C, 74.79; H, 6.43; N, 8.95.

2-Allyl-6-morpholin-4-yl-benzo[de]isoquinoline-1,3-dione (**6b**)³²

Yellow solid (87 %); m.p. 173-174 °C; ¹H NMR (400 MHz, CDCl₃): δ 8.61 (dd, ²J = 7.32 Hz, ³J = 1.40 Hz, 1H, ArH), 8.55 (d, ²J = 8.24 Hz, 1H, ArH), 8.44 (dd, ²J = 8.68 Hz, ³J = 1.36 Hz, 1H, ArH), 7.73 (dd, ²J = 8.24 Hz, ³J = 7.32 Hz, 1H, ArH), 7.27 (t, ²J = 9.36 Hz, 1H, ArH), 6.04-5.94 (m, 1H, CH), 5.33-5.28 (dq, ²J = 17.42 Hz, ³J = 1.36 Hz, 1H, CH₂), 5.21-5.18 (dq, ²J = 10.08 Hz, ³J = 1.36 Hz, 1H, CH₂), 4.81-4.78 (dt, ²J = 5.96 Hz, ³J = 1.36 Hz,

2H, N-CH₂), 4.03 (t, ²J = 4.12 Hz, 4H, mor-CH₂), 3.27 (t, ²J = 4.60 Hz, 4H, mor-CH₂); ¹³C NMR (100 MHz, CDCl₃): δ 161.3 (C=O), 160.8 (C=O), 152.9, 129.8, 129.5, 128.5, 127.3, 127.1, 123.3, 123.0, 120.4, 114.5, 114.2, 112.1 (ArC), 64.1 (mor-OCH₂), 50.6 (mor-NCH₂), 39.5 (N-CH₂); MS (EI) : m/z 323.1 (M⁺+1). Anal. Calc. for C₁₉H₁₈N₂O₃: C, 70.79; H, 5.63; N, 8.69. Found: C, 70.55; H, 5.89; N, 8.83.

2-Allyl-6-pyrrolidin-1-yl-benzo[de]isoquinoline-1,3-dione (**6c**)

Yellow solid (76 %); m.p. 155-158 °C; ¹H NMR (400 MHz, CDCl₃): δ 8.59-8.55 (m, 2H, ArH), 8.42 (d, ²J = 8.68 Hz, 1H, ArH), 7.54 (dd, ²J = 8.68 Hz, ³J = 1.32 Hz, 1H, ArH), 6.80 (d, ²J = 8.68 Hz, 1H, ArH), 6.05-5.96 (m, 1H, CH), 5.31-5.26 (dq, ²J = 16.96 Hz, ³J = 1.36 Hz, 1H, CH₂), 5.19-5.16 (dq, ²J = 10.54 Hz, ³J = 1.36 Hz, 1H, CH₂), 4.81-4.79 (dt, ²J = 5.48 Hz, ³J = 1.36 Hz, 2H, N-CH₂), 3.78 (t, ²J = 6.44 Hz, 4H, pyr-CH₂), 2.11-2.08 (m, 4H, pyr-CH₂); ¹³C NMR (100 MHz, CDCl₃): δ 164.4 (C=O), 163.6 (C=O), 152.5, 133.4, 132.6, 131.9, 131.0, 122.8, 122.3, 122.2, 116.8, 110.1, 108.3 (ArC), 53.0 (pyr-CH₂), 42.0 (N-CH₂), 25.9 (pyr-CH₂); MS (EI) : m/z 307.1 (M⁺+1). Anal. Calc. for C₁₉H₁₈N₂O₂: C, 74.49; H, 5.92; N, 9.14. Found: C, 74.78; H, 5.77; N, 9.36.

2-Allyl-6-(4-amino-phenylsulfanyl)-benzo[de]isoquinoline-1,3-dione (**6d**)

Brown solid (60 %); m.p. 185-188 °C; ¹H NMR (400 MHz, CDCl₃): δ 8.65-8.61 (m, 2H, ArH), 8.31 (d, ²J = 8.24 Hz, 1H, ArH), 7.79 (dd, ²J = 8.24 Hz, ³J = 7.32 Hz, 1H, ArH), 7.40 (d, ²J = 8.72 Hz, 2H, ArH), 7.06 (d, ²J = 7.76 Hz, 1H, ArH), 6.81 (d, ²J = 8.68 Hz, 2H, ArH), 6.01-5.95 (m, 1H, CH), 5.32-5.26 (dq, ²J = 17.42 Hz, ³J = 1.36 Hz, 1H, CH₂), 5.21-5.17 (dq, ²J = 10.08 Hz, ³J = 1.36 Hz, 1H, CH₂), 4.79-4.77 (dt, ²J = 5.48 Hz, ³J = 1.36 Hz, 2H, N-CH₂), 4.01 (bs, 2H, NH₂); ¹³C NMR (100 MHz, CDCl₃): δ 163.8 (C=O), 163.7 (C=O), 148.8, 148.3, 137.4, 132.1, 131.6, 131.0, 129.8, 128.3, 126.5, 122.9, 122.8, 118.5, 117.3, 116.3, 115.5 (ArC), 42.3 (N-CH₂); MS (EI) : m/z 361.1 (M⁺+1). Anal. Calc. for C₂₁H₁₆N₂O₂S: C, 69.98; H, 4.47; N, 7.77; S, 8.90. Found: C, 69.83; H, 4.69; N, 7.52; S, 8.73.

2-Allyl-6-(2-amino-phenylsulfanyl)-benzo[de]isoquinoline-1,3-dione (**6e**)

Yellow solid (59 %); m.p. 205-208 °C; ¹H NMR (400 MHz, CDCl₃): δ 8.49 (q, ²J = 8.28 Hz, 2H, ArH), 8.11 (d, ²J = 7.80 Hz, 1H, ArH), 7.72-7.62 (m, 3H, ArH), 7.57 (d, ²J = 8.24 Hz, 1H, ArH), 7.47 (t, ²J = 7.76 Hz, 1H, ArH), 6.82 (d, ²J = 8.24 Hz, 1H, ArH), 5.90-5.82 (m, 1H, CH), 5.24 (d, ²J = 16.96 Hz, 1H, CH₂), 5.17 (d, ²J = 10.08 Hz, 1H, CH₂), 4.64 (d, ²J = 5.96 Hz, 2H, N-CH₂); ¹³C NMR (100 MHz, CDCl₃): δ 161.4 (C=O), 161.3 (C=O), 148.9, 143.1, 135.7, 130.7, 130.5, 129.7, 129.0, 128.2, 126.7, 126.4, 125.3, 120.8, 120.5, 116.8, 116.0, 115.0, 113.9, 106.6 (ArC), 42.3 (N-CH₂); MS (EI) : m/z 361.1 (M⁺+1). Anal. Calc. for C₂₁H₁₆N₂O₂S: C, 69.98; H, 4.47; N, 7.77; S, 8.90. Found: C, 69.79; H, 4.64; N, 7.99; S, 8.65.

2-Allyl-6-(3-hydroxy-pyridin-2-ylamino)-benzo[de]isoquinoline-1,3-dione (**6f**)

Yellow solid (63 %); m.p. 210-212 °C; ¹H NMR (400 MHz, CDCl₃): δ 8.70 (d, ²J = 8.72 Hz, 1H, ArH), 8.65 (d, ²J = 7.36 Hz, 1H, ArH), 8.48 (dd, ²J = 8.24 Hz, ³J = 0.92 Hz, 1H, ArH), 8.06 (d, ²J = 5.04 Hz, 1H, ArH), 7.82 (t, ²J = 7.56 Hz, 1H, ArH), 7.29-7.27

(m, 1H, ArH), 6.94 (dd, $^2J = 8.24$ Hz, $^3J = 0.92$ Hz, 1H, ArH), 6.79-6.75 (m, 1H, ArH), 6.02-5.94 (m, 1H, CH), 5.33-5.29 (dt, $^2J = 16.96$ Hz, $^3J = 1.36$ Hz, 1H, CH₂), 5.22-5.20 (dt, $^2J = 10.08$ Hz, $^3J = 1.40$ Hz, 1H, CH₂), 4.80-4.77 (m, 2H, N-CH₂); ¹³C NMR (100 MHz, CDCl₃): δ 163.8 (C=O), 163.2 (C=O), 158.1, 151.8, 145.0, 136.4, 132.9, 132.1, 129.6, 128.4, 128.1, 126.8, 123.5, 122.5, 117.5, 117.1, 114.5, 109.8 (ArC), 42.3 (N-CH₂); MS (EI) : m/z 346.1 (M⁺+1). Anal. Calc. for C₂₀H₁₅N₃O₃: C, 69.56; H, 4.38; N, 12.17. Found: C, 69.33; H, 4.54; N, 12.43.

10 **2-Allyl-6-(5-bromo-pyridin-2-ylamino)-benzo[de]isoquinoline-1,3-dione (6g)**

Brown solid (53 %); m.p. 205-207 °C; ¹H NMR (400 MHz, CDCl₃): δ 8.75 (dd, $^2J = 8.68$ Hz, $^3J = 1.36$ Hz, 1H, ArH), 8.67 (dd, $^2J = 7.32$ Hz, $^3J = 1.36$ Hz, 1H, ArH), 8.45 (d, $J = 8.24$ Hz, 1H, ArH), 7.79 (dd, $^2J = 8.68$ Hz, $^3J = 1.36$ Hz, 1H, ArH), 7.01 (d, $J = 1.96$ Hz, 2H, ArH), 6.86 (d, $J = 8.24$ Hz, 1H, ArH), 6.79 (d, $J = 8.68$ Hz, 1H, ArH), 6.04-5.95 (m, 1H, CH), 5.33-5.28 (dq, $^2J = 17.18$ Hz, $^3J = 1.36$ Hz, 1H, CH₂), 5.22-5.18 (dq, $^2J = 10.08$ Hz, $^3J = 1.36$ Hz, 1H, CH₂), 4.81-4.79 (dt, $^2J = 5.96$ Hz, $^3J = 1.36$ Hz, 2H, N-CH₂); ¹³C NMR (100 MHz, CDCl₃): δ 164.2 (C=O), 163.5 (C=O), 161.1, 146.1, 144.2, 133.1, 132.3, 131.9, 129.6, 128.8, 126.2, 123.6, 122.3, 122.0, 117.2, 116.3, 115.6, 109.3 (ArC), 42.2 (N-CH₂); MS (EI) : m/z 345.1 (M⁺+1). Anal. Calc. for C₂₀H₁₄BrN₃O₂: C, 58.84; H, 3.46; N, 10.29. Found: C, 58.49; H, 3.65; N, 10.07.

2-Allyl-6-(2-hydroxy-ethylamino)-benzo[de]isoquinoline-1,3-dione (6h)

Brown liquid (57 %); ¹H NMR (400 MHz, CDCl₃): δ 8.56 (d, $J = 7.32$ Hz, 1H, ArH), 8.44 (d, $J = 8.68$ Hz, 1H, ArH), 8.35 (d, $J = 8.28$ Hz, 1H, ArH), 7.61 (t, $J = 8.24$ Hz, 1H, ArH), 6.70 (d, $J = 8.72$ Hz, 1H, ArH), 6.34 (t, $J = 4.36$ Hz, 1H, NH), 6.01-5.96 (m, 1H, CH), 5.31-5.25 (dq, $^2J = 17.4$ Hz, $^3J = 1.40$ Hz, 1H, CH₂), 5.19-5.16 (dq, $^2J = 10.3$ Hz, $^3J = 1.40$ Hz, 1H, CH₂), 4.79-4.77 (dt, $^2J = 5.48$ Hz, $^3J = 1.84$ Hz, 2H, N-CH₂), 4.21 (bs, 1H, OH), 4.00 (t, $J = 4.60$ Hz, 2H, CH₂), 3.53 (q, $J = 5.04$ Hz, 2H, CH₂); ¹³C NMR (100 MHz, CDCl₃): δ 164.3 (C=O), 163.8 (C=O), 163.9, 163.2, 158.0, 151.7, 149.4, 144.9, 136.4, 134.4, 132.9, 132.5, 132.1, 131.3, 129.7, 128.4, 128.1, 126.8, 126.1, 124.8, 123.5, 122.8, 122.5, 117.5, 117.2, 117.0, 114.5, 110.4, 109.9, 104.4 (ArC), 60.4 (O-CH₂), 45.2 (N-CH₂), 42.3 (N-CH₂); MS (EI) : m/z 297.0 (M⁺+1). Anal. Calc. for C₁₇H₁₆N₂O₃: C, 68.91; H, 5.44; N, 9.45. Found: C, 68.76; H, 5.79; N, 9.22.

2-Allyl-6-allylamino-benzo[de]isoquinoline-1,3-dione (6i)

Brown liquid (50 %); ¹H NMR (400 MHz, CDCl₃): δ 8.59 (d, $J = 7.32$ Hz, 1H, ArH), 8.47 (d, $J = 8.72$ Hz, 1H, ArH), 8.14 (d, $J = 8.72$ Hz, 1H, ArH), 7.64 (t, $J = 8.28$ Hz, 1H, ArH), 6.73 (d, $J = 8.72$ Hz, 1H, ArH), 6.04-5.96 (m, 2H, CH), 5.49 (bs, 1H, NH), 5.41-5.16 (m, 4H, CH₂), 4.80 (dd, $^2J = 5.96$ Hz, $^3J = 1.36$ Hz, 2H, N-CH₂), 4.09 (t, $J = 5.28$ Hz, 2H, N-CH₂); ¹³C NMR (100 MHz, CDCl₃): δ 164.4 (C=O), 163.8 (C=O), 149.0, 134.5, 132.9, 132.5, 131.2, 118.0, 116.9, 104.9 (ArC), 46.0 (N-CH₂), 42.1 (N-CH₂); MS (EI) : m/z 293.1 (M⁺+1). Anal. Calc. for C₁₈H₁₆N₂O₂: C, 73.95; H, 5.52; N, 9.58. Found: C, 73.63; H, 5.70; N, 9.34.

2-Allyl-6-propylamino-benzo[de]isoquinoline-1,3-dione (6j)

Yellow liquid (80 %); ¹H NMR (400 MHz, CDCl₃): δ 8.58 (dd, $^2J = 7.32$ Hz, $^3J = 0.92$ Hz, 1H, ArH), 8.46 (d, $J = 8.24$ Hz, 1H,

ArH), 8.11 (d, $J = 7.80$ Hz, 1H, ArH), 7.61 (dd, $^2J = 8.28$ Hz, $^3J = 0.92$ Hz, 1H, ArH), 6.72 (d, $J = 8.72$ Hz, 1H, ArH), 6.03-5.97 (m, 1H, CH), 5.36 (bs, 1H, NH), 5.31-5.26 (dq, $^2J = 17.16$ Hz, $^3J = 1.40$ Hz, 1H, CH₂), 5.19-5.16 (dq, $^2J = 10.52$ Hz, $^3J = 1.40$ Hz, 1H, CH₂), 4.80 (dt, $^2J = 5.48$ Hz, $^3J = 1.36$ Hz, 2H, N-CH₂), 3.40-3.35 (m, 2H, prop-NCH₂), 1.87-1.81 (m, 2H, prop-CH₂), 1.11 (t, $J = 7.36$ Hz, 3H, prop-CH₃); ¹³C NMR (100 MHz, CDCl₃): δ 164.4 (C=O), 163.8 (C=O), 149.5, 134.6, 132.6, 131.2, 129.8, 125.8, 124.6, 122.9, 120.0, 116.9, 109.9, 104.3 (ArC), 45.4 (N-CH₂), 42.1 (N-CH₂), 22.1 (CH₂), 11.6 (CH₃); MS (EI) : m/z 295.1 (M⁺+1). Anal. Calc. for C₁₈H₁₈N₂O₂: C, 73.45; H, 6.16; N, 9.52. Found: C, 73.72; H, 6.30; N, 9.31.

2-Allyl-6-butylamino-benzo[de]isoquinoline-1,3-dione (6k)

Yellow liquid (62 %); ¹H NMR (400 MHz, CDCl₃): δ 8.58 (dd, $^2J = 7.32$ Hz, $^3J = 0.92$ Hz, 1H, ArH), 8.47 (d, $J = 8.24$ Hz, 1H, ArH), 8.10 (dd, $^2J = 8.24$ Hz, $^3J = 0.92$ Hz, 1H, ArH), 7.62 (dd, $^2J = 8.72$ Hz, $^3J = 1.32$ Hz, 1H, ArH), 6.72 (d, $J = 8.68$ Hz, 1H, ArH), 6.03-5.97 (m, 1H, CH), 5.31-5.26 (dq, $^2J = 17.18$ Hz, $^3J = 1.36$ Hz, 1H, CH₂), 5.19-5.16 (dq, $^2J = 10.08$ Hz, $^3J = 1.40$ Hz, 1H, CH₂), 4.80-4.78 (dt, $^2J = 5.96$ Hz, $^3J = 1.36$ Hz, 2H, N-CH₂), 3.43-3.38 (m, 2H, but-NCH₂), 1.84-1.75 (m, 2H, but-CH₂), 1.56-1.50 (m, 2H, but-CH₂), 1.04 (t, $J = 7.32$ Hz, 3H, but-CH₃); ¹³C NMR (100 MHz, CDCl₃): δ 164.4 (C=O), 163.8 (C=O), 149.5, 134.6, 132.6, 131.2, 129.8, 125.8, 124.6, 122.9, 120.0, 116.9, 109.9, 104.2 (ArC), 43.3 (but-NCH₂), 42.1 (N-CH₂), 30.9 (but-CH₂), 20.3 (but-CH₂), 13.8 (but-CH₃); MS (EI) : m/z 309.2 (M⁺+1). Anal. Calc. for C₁₉H₂₀N₂O₂: C, 74.00; H, 6.54; N, 9.08. Found: C, 74.33; H, 6.29; N, 9.37.

2-Allyl-6-pentylamino-benzo[de]isoquinoline-1,3-dione (6l)

Yellow liquid (59 %); ¹H NMR (400 MHz, CDCl₃): δ 8.59 (dd, $^2J = 7.32$ Hz, $^3J = 0.92$ Hz, 1H, ArH), 8.47 (d, $J = 8.24$ Hz, 1H, ArH), 8.10 (dd, $^2J = 8.24$ Hz, $^3J = 0.92$ Hz, 1H, ArH), 7.63 (dd, $^2J = 8.68$ Hz, $^3J = 7.32$ Hz, 1H, ArH), 6.72 (d, $J = 8.24$ Hz, 1H, ArH), 6.03-5.97 (m, 1H, CH), 5.31-5.26 (dq, $^2J = 17.18$ Hz, $^3J = 1.36$ Hz, 1H, CH₂), 5.19-5.16 (dq, $^2J = 10.08$ Hz, $^3J = 1.40$ Hz, 1H, CH₂), 4.80-4.78 (dt, $^2J = 5.48$ Hz, $^3J = 1.36$ Hz, 2H, N-CH₂), 3.42-3.37 (m, 2H, pent-NCH₂), 1.85-1.78 (m, 2H, pent-CH₂), 1.50-1.38 (m, 4H, pent-CH₂), 0.97 (t, $J = 7.36$ Hz, 3H, pent-CH₃); ¹³C NMR (100 MHz, CDCl₃): δ 164.4 (C=O), 163.8 (C=O), 149.5, 134.6, 132.6, 131.2, 129.8, 125.8, 124.6, 122.9, 120.1, 116.9, 109.9, 104.3 (ArC), 43.6 (pent-NCH₂), 42.1 (N-CH₂), 29.2 (pent-CH₂), 28.6 (pent-CH₂), 22.4 (pent-CH₂), 13.9 (pent-CH₃); MS (EI) : m/z 323.2 (M⁺+1). Anal. Calc. for C₂₀H₂₂N₂O₂: C, 74.51; H, 6.88; N, 8.69. Found: C, 74.68; H, 6.59; N, 8.57.

2-Allyl-6-hexylamino-benzo[de]isoquinoline-1,3-dione (6m)

Yellow liquid (51 %); ¹H NMR (400 MHz, CDCl₃): δ 8.61 (dd, $^2J = 7.76$ Hz, $^3J = 1.36$ Hz, 1H, ArH), 8.49 (d, $J = 8.24$ Hz, 1H, ArH), 8.09 (d, $J = 7.80$ Hz, 1H, ArH), 7.65 (dd, $^2J = 8.24$ Hz, $^3J = 1.32$ Hz, 1H, ArH), 6.74 (d, $J = 8.28$ Hz, 1H, ArH), 6.04-5.95 (m, 1H, CH), 5.32-5.26 (dq, $^2J = 17.2$ Hz, $^3J = 1.36$ Hz, 1H, CH₂), 5.20-5.16 (dq, $^2J = 10.08$ Hz, $^3J = 1.36$ Hz, 1H, CH₂), 4.80-4.78 (dt, $^2J = 5.52$ Hz, $^3J = 1.36$ Hz, 2H, N-CH₂), 3.43-3.38 (m, 2H, hex-NCH₂), 1.85-1.78 (m, 2H, hex-CH₂), 1.52-1.46 (m, 2H, hex-CH₂), 1.38-1.36 (m, 4H, hex-CH₂), 0.94-0.91 (m, 3H, hex-CH₃); ¹³C NMR (100 MHz, CDCl₃): δ 164.4 (C=O), 163.8 (C=O), 149.4, 134.6, 132.6, 131.2, 129.8, 125.8, 124.6, 123.0, 120.1, 116.9, 110.0, 104.3 (ArC), 43.7 (hex-NCH₂), 42.1 (N-CH₂), 31.5 (hex-CH₂), 28.9 (hex-CH₂), 26.8 (hex-CH₂), 22.5 (hex-CH₂), 14.0

(hex-CH₃); MS (EI) : m/z 337.2 (M⁺+1). Anal. Calc. for C₂₃H₂₄N₂O₂: C, 74.97; H, 7.19; N, 8.33. Found: C, 74.67; H, 7.32; N, 8.47.

2-Allyl-6-octylamino-benzo[de]isoquinoline-1,3-dione (6n)

Yellow liquid (49 %); ¹H NMR (400 MHz, CDCl₃): δ 8.54 (d, *J* = 7.36 Hz, 1H, ArH), 8.43 (d, *J* = 8.24 Hz, 1H, ArH), 8.13 (d, *J* = 8.24 Hz, 1H, ArH), 7.57 (t, *J* = 8.04 Hz, 1H, ArH), 6.68 (d, *J* = 8.72 Hz, 1H, ArH), 6.03-5.96 (m, 1H, CH), 5.53 (t, *J* = 4.8 Hz, 1H, NH), 5.31-5.26 (dq, ²*J* = 17.42 Hz, ³*J* = 1.36 Hz, 1H, CH₂), 5.19-5.15 (dq, ²*J* = 10.08 Hz, ³*J* = 1.36 Hz, 1H, CH₂), 4.79 (d, *J* = 5.52 Hz, 2H, N-CH₂), 3.40-3.35 (m, 2H, octyl-NCH₂), 1.83-1.76 (m, 2H, octyl-CH₂), 1.51-1.44 (m, 2H, octyl-CH₃), 1.38-1.25 (m, 8H, octyl-CH₂), 0.89 (t, *J* = 6.88 Hz, 3H, octyl-CH₃); ¹³C NMR (100 MHz, CDCl₃): δ 164.3 (C=O), 163.7 (C=O), 149.6, 134.5, 132.5, 131.1, 129.7, 126.0, 124.4, 122.7, 120.0, 116.9, 109.6, 104.1 (ArC), 43.6 (octyl-NCH₂), 42.0 (N-CH₂), 31.7 (octyl-CH₂), 29.2 (octyl-CH₂), 29.1 (octyl-CH₂), 28.8 (octyl-CH₂), 27.1 (octyl-CH₂), 22.5 (octyl-CH₂), 14.0 (octyl-CH₃); MS (EI) : m/z 365.2 (M⁺+1). Anal. Calc. for C₂₃H₂₈N₂O₂: C, 75.79; H, 7.74; N, 7.69. Found: C, 75.95; H, 7.89; N, 7.53.

4.4. *In vitro* evaluation assay

In vitro anticancer screening at NCI is a two-stage process, beginning with the evaluation of all compounds against the 60 cell lines at a single dose of 10 μM. The output from the single dose screen is reported as a mean graph and is available for analysis by the COMPARE program. Compounds which exhibit significant growth inhibition are evaluated against the 60 cell panel at five concentration levels. The human tumor cell lines of the cancer screening panel are grown in RPMI 1640 medium containing 5% fetal bovine serum and 2 mM L-glutamine. For a typical screening experiment, cells are inoculated into 96 well microtiter plates in 100 mL at plating densities ranging from 5000 to 40,000 cells/well depending on the doubling time of individual cell lines. After cell inoculation, the microtiter plates are incubated at 37° C, 5% CO₂, 95% air and 100% relative humidity for 24 h prior to addition of experimental drugs.

After 24 h, two plates of each cell line are fixed *in situ* with TCA, to represent a measurement of the cell population for each cell line at the time of drug addition (Tz). Experimental drugs are solubilized in dimethyl sulfoxide at 400 fold the desired final maximum test concentration and stored frozen prior to use. At the time of drug addition, an aliquot of frozen concentrate is thawed and diluted to twice the desired final maximum test concentration with complete medium containing 50 μg/ml gentamicin. Additional four, 10-fold or ½ log serial dilutions are made to provide a total of five drug concentrations plus control. Aliquots of 100 μL of these different drug dilutions are added to the appropriate microtiter wells already containing 100 μL of medium, resulting in the required final drug concentrations. Following drug addition, the plates are incubated for an additional 48 h at 37° C, 5% CO₂, 95% air, and 100% relative humidity. For adherent cells, the assay is terminated by the addition of cold TCA. Cells are fixed *in situ* by the gentle addition of 50 μL of cold 50% (w/v) TCA (final concentration, 10% TCA) and incubated for 60 min at 4° C. The supernatant is discarded, and the plates are washed five times with tap water and air dried. Sulforhodamine B (SRB) solution (100 μl) at 0.4% (w/v) in 1% acetic acid is added to each well, and plates are incubated for 10 min at room temperature. After staining, unbound dye is removed by washing five times with 1% acetic

acid and the plates are air dried. Bound stain is subsequently solubilized with 10 mM trizma base, and the absorbance is read on an automated plate reader at a wavelength of 515 nm. For suspension cells, the methodology is the same except that the assay is terminated by fixing settled cells at the bottom of the wells by gently adding 50 μL of 80% TCA (final concentration, 16% TCA). Using the seven absorbance measurements [time zero, (Tz), control growth, (C), and test growth in the presence of drug at the five concentration levels (Ti)], the percentage growth is calculated at each of the drug concentrations levels. Percentage growth inhibition is calculated as:

$$[(Ti - Tz)/(C-Tz)] \times 100 \text{ for concentrations for which } Ti \geq Tz$$

$$[(Ti - Tz)/Tz] \times 100 \text{ for concentrations for which } Ti < Tz:$$

Three dose response parameters are calculated for each experimental agent. Growth inhibition of 50% (GI₅₀) is calculated from $[(Ti-Tz)/(C-Tz)] \times 100 = 50$, which is the drug concentration resulting in a 50% reduction in the net protein increase (as measured by SRB staining) in control cells during the drug incubation. The drug concentration resulting in total growth inhibition (TGI) is calculated from $Ti = Tz$. The LC₅₀ (concentration of drug resulting in a 50% reduction in the measured protein at the end of the drug treatment as compared to that at the beginning) indicating a net loss of cells following treatment is calculated from $[(Ti-Tz) / Tz] \times 100 = -50$. Values are calculated for each of these three parameters if the level of activity is reached; however, if the effect is not reached or is exceeded, the value for that parameter is expressed as greater or less than the maximum or minimum concentration tested.

4.5. MTT assay

Hek293 (Human embryonic kidney) cells, DMEM with 50mM glutamine, 10% FBS, 100 U/ml penicillin and 100 mg/ml streptomycin. The test was performed against Hek293 (Human embryonic kidney) cells. Cells were seeded in 96 well plates at the density of 1x10⁵ cells/well in DMEM media supplemented with 10% FBS cells. Cells were incubated at 37 °C in 5% CO₂ incubator. Cells were treated with compound **6b** at five concentrations (10⁻⁴, 10⁻⁵, 10⁻⁶, 10⁻⁷, 10⁻⁸ M) for 24 h at 37 °C. 10 μl of MTT (prepared in 1* PBS buffer) from 5 mg/ml stock was added in each well and incubated at 37 °C for 4 h in dark. The formazan crystals were dissolved using 100 μl of DMSO. Further, the amount of formazan crystal formation was measured as difference in absorbance by Bio-Red ELISA plate reader at 570 nm and 690 nm reference wavelength. The relative cell toxicity (%) related to control wells containing culture medium without test material was calculated by using formula:

$$\% \text{ Cell Toxicity} = 100 - \frac{\text{OD (Compound treated wells)}}{\text{OD (Untreated Wells)}} \times 100$$

4.6. LDH activity

A549 cells (5x10⁶ cells/well) were seeded in 96 well plates with DMEM (Biological Industries) media contains 10% FBS (Sigma-Aldrich) and 1% PenStrep (Sigma-Aldrich), incubated at 37 °C in 5% CO₂ incubator. Cells were allowed to adhere. After 24 h, containing media was replaced by fresh media and treated with mentioned concentration of compound again

following incubation for 12 and 24 h respectively in 5%CO₂ incubator at 37°C. Removal of aliquot of the culture medium form seeded cell followed by the addition of Lactate Dehydrogenase assay mixture (LDH assay substrate solution, LDH assay dye solution, and 1× LDH assay cofactor) into each sample in a volume equal to twice. Plates were covered with aluminum foil to protect from light and incubated at room temperature for 20–30 minutes. After incubation reaction was terminated by the addition of 1/10 volume of 1 N HCl to each well. Absorbance measured at wavelength of 490 nm by ELISA reader. Measure absorbance of the blank was subtracted from this value.

4.7. DNA binding studies

Stock solution of compound **6b** (1 mM) was prepared by dissolving **6b** in AR grade DMSO. The DNA binding experiments were carried out by making dilution of stock solution with phosphate buffer. Stock solution of ct-DNA was prepared by dissolving DNA in phosphate buffer (10 mM, pH 7.0). The DNA concentration was estimated from its absorbance intensity at 260 nm with a known molar absorption coefficient value of 6600 dm³M⁻¹cm⁻¹. The purity of DNA was established from ratio of absorbance intensity at 260 nm and at 280 nm.

UV-Vis and Fluorescence titrations: The titration experiments were performed by varying the concentration of ct-DNA and keeping the compound concentration constant (20 μM). All the UV spectra were recorded after equilibration of solution for 5 min. Fluorescence titration were carried out on Cary Eclipse Fluorescence Spectrophotometer at ambient temperature. A slit width of 10 nm was used with λ_{ex} = 400 nm. The titration experiment was accomplished by varying the concentration of DNA in cuvette (0.5-150 μM).

DNA thermal denaturation: DNA melting experiments were carried out by observing the absorbance of ct-DNA at 280 nm at various temperature in the absence and presence of compound with a ramp rate of 0.5 °C/min in a phosphate buffer (pH 7.0) on a Shimadzu Spectrophotometer equipped with a Peltier thermo regulator.

Acknowledgements

We thank Department of Science and Technology, New Delhi (SR/FT/CS-40/2010) for the research grant. We also thank SAI Labs, Thapar University, Patiala for recording NMR spectra and Punjab University, Chandigarh for recording mass spectra. NCI, USA and Institute for Industrial research and toxicology (IIRT), India is gratefully acknowledged for investigating antitumour activities. We also thank Dr. N. Tejo Prakash for his valuable guidance.

References and notes

- (a) S. Neidle and D. E. Thurston, *Nat. Rev. Cancer*, 2005, **5**, 285. (b) K. Ninomiya, H. Satoh, T. Sugiyama, M. Shinomiya and R. Kuroda, *Chem. Commun.*, 1996, 1825. (c) Y. H. Du, J. Huang, X. C. Weng and X. Zhou, *Curr. Med. Chem.: Anti-Cancer Agents*, 2010, **17**, 173. (d) G. Bischoff and S. Hoffmann, *Curr. Med. Chem.: Anti-Cancer Agents*, 2002, **9**, 321. (e) L. H. Hurley, *Nat. Rev. Cancer*, 2002, **2**, 188.
- M. F. Brana and A. Ramos, *Curr. Med. Chem.: Anti-cancer Agents*, 2001, **1**, 237.

- E. Van Quaquebeke, T. Mahieu, P. Dumont, J. Dewelle, F. Ribaucour, G. Simon, S. Sauvage, J. F. Gaussin, J. Tuti, M. El Yazidi, F. Van Vynckt, T. Mijatovic, F. Lefranc, F. Darro and R. Kiss, *J. Med. Chem.*, 2007, **50**, 4122.
- (a) V. K. Malviya, P. Y. Liu, D. S. Alberts, E. A. Surwit, J. B. Craig and E. V. Hannigan, *Am. J. Clin. Oncol.*, 1992, **15**, 41. (b) I. Ott, X. Qian, Y. Xu, D. H. W. Vlecken, I. J. Marques, D. Kubutat, J. Will, W. S. Sheldrick, P. Jesse, A. Prokop and C. P. Bagowski, *J. Med. Chem.*, 2009, **52**, 763.
- R. Rosell, J. Carles, A. Abad, N. Ribelles, A. Barnadas, A. Benavides and M. Martin, *Invest. New Drugs*, 1992, **10**, 171.
- M. F. Brana, M. Cacho, M. A. Garcia, B. de Pascual-Teresa, A. Ramos, N. Acero, F. Llinares, D. Munoz-Mingarro, C. Abradelo, M. F. Rey-Stolle and M. Yuste, *J. Med. Chem.*, 2002, **45**, 5813.
- U. Hossain Sk, A. S. P. Gowda, M. A. Crampsie, J. K. Yun, T. E. Spratt, S. Amin and A. K. Sharma, *Eur. J. Med. Chem.*, 2011, **46**, 3331.
- M. J. Ratain, R. Mick, F. Berezin, L. Janisch, R. L. Schilsky, N. J. Vogelzang and L.B. Lane, *Cancer Res.* 1993, **53**, 2304.
- Q. Yang, P. Yang, X. Qian and L. Tong, *Bioorg. Med. Chem. Lett.*, 2008, **18**, 6210
- M. Verma, V. Luxami and K. Paul, *Eur. J. Med. Chem.*, 2013, **68**, 352.
- (a) K. Wang, Y. Wang, X. Yan, H. Chen, G. Ma, P. Zhang, J. Li, X. Li and J. Zhang, *Bioorg. Med. Chem. Lett.*, 2012, **22**, 937. (b) L. Xie, J. Cui, X. Qian, Y. Xu, J. Liu and R. Xu, *Bioorg. Med. Chem.*, 2011, **19**, 961.
- X. Li, Y. Lin, Q. Wang, Y. Yuan, H. Zhang and X. Qian, *Eur. J. Med. Chem.*, 2011, **46**, 1274.
- X. Li, Y. Lin, Y. Yuan, K. Liu and X. Qian, *Tetrahedron*, 2011, **67**, 2299.
- K.-R. Wang, F. Qian, X.-M. Wang, G.-H. Tan, R.-X. Rong, Z.-R. Cao, H. Chen, P.-Z. Zhang and X.-L. Li, *Chin. Chem. Lett.*, 2014, **25**, 1087.
- T. Mijatovic, T. Mahieu, C. Bruyère, N. De Nève, J. Dewelle, G. Simon, M. J. M. Dehoux, E. v. Aar, B. Haibe-Kains, G. Bontempi, C. Decaestecker, E. V. Quaquebeke, F. Darro and R. Kiss, *Neoplasia*, 2008, **10**, 573.
- Z. Li, Q. Yang and X. Qian, *Tetrahedron*, 2005, **61**, 6634.
- R. Martinez, L. Chacon-Garcia, *Curr. Med. Chem.* 2005, **12**, 127.
- S. Banerjee, E. B. Veale, C. M. Phelan, S. A. Murphy, G. M. Tocci, L. J. Gillespie, D. O. Frimannsson, J. M. Kelly and T. Gunnlaugsson, *Chem. Soc. Rev.* 2013, **42**, 1601.
- M. R. Grever, S. A. Sehepartz and B. A. Chabners, *Semin. Oncol.*, 1992, **19**, 622.
- A. Monks, D. Schudiero, P. Skehan, R. Shoemaker, K. Paull, D. Vistica, C. Hose, J. Langley, P. Cronise, A. Vaigro-Wolf, M. Gray-Goodrich, H. Campbell, J. Mayo and M. J. Boyd, *Natl. Cancer Inst.*, 1991, **83**, 757.
- M. R. Boyd and K. D. Paull, *Drug Dev. Res.*, 1995, **34**, 91.
- (a) N. J. Wheate, S. Walker, G. E. Craig and R. Oun, *Dalton Trans.*, 2010, **39**, 8113. (b) O. M. Alian, A. S. Azmi and R. M. Mohammad, *Clin. Transl. Med.*, 2012, **1**, 26.
- G. Belmadani, A. M. Tramu, P. S. Betbeder and E. E. Steyn, *Arch. Toxicol.*, 1998, **72**, 656.
- S. Tan, H. Yin, Z. Chen, X. Qian and Y. Xu, *Eur. J. Med. Chem.*, 2013, **62**, 130.
- Mudasir, E. T. Wahyuni, D. H. Tjahjono, N. Yosioka, H. Inoue, *Spectrochim. Acta Part A*, 2010, **77**, 528.
- J. M. Ruso, D. Attwood, M. Garcia, P. Taboada, L. M. Varela and V. Mosquera, *Langmuir*, 2001, **17**, 5189. (b) T. Banerjee, S. K. Singh and N. Kishore, *J. Phys. Chem. B*, 2006, **110**, 24147.
- G. Vistoli, A. Pedretti and B. Testa, *Drug Discovery Today*, 2008, **13**, 285.
- C. A. Lipinski, F. Lombardo, B. W. Dominy and P. J. Feeney, *Adv. Drug Delivery Rev.*, 2001, **46**, 3.
- R. Rohs, I. Bloch, H. Sklenar and Z. Shakked, *Nucleic Acids Res.*, 2005, **33**, 7048.
- Compounds were constructed and docked with builder toolkit of the software package ArgusLab 4.0.1 (www.arguslab.com).
- <http://pubchem.ncbi.nlm.nih.gov/assay/assay.cgi?aid=602473>.

-
32. R. H. Guenther, S. P. Yenne and J. R. Szewczyk, 'Screening methods for identifying specific staphylococcus aureus inhibitors' *US Pat.*, 0163037, 2014.

5